

Quantum Phase Transition and Emergent Symmetry in a Quadruple Quantum Dot System

Dong E. Liu, Shailesh Chandrasekharan, and Harold U. Baranger

Department of Physics, Duke University, Box 90305, Durham, North Carolina 27708-0305, USA

(Received 6 August 2010; published 13 December 2010)

We propose a system of four quantum dots designed to study the competition between three types of interactions: Heisenberg, Kondo, and Ising. We find a rich phase diagram containing two sharp features: a quantum phase transition (QPT) between charge-ordered and charge-liquid phases and a dramatic resonance in the charge liquid visible in the conductance. The QPT is of the Kosterlitz-Thouless type with a discontinuous jump in the conductance at the transition. We connect the resonance phenomenon with the degeneracy of three levels in the isolated quadruple dot and argue that this leads to a Kondo-like emergent symmetry from left-right Z_2 to $U(1)$.

DOI: 10.1103/PhysRevLett.105.256801

PACS numbers: 73.21.La, 05.30.Rt, 72.10.Fk, 73.23.Hk

Strong electronic correlations create a variety of interesting phenomena including quantum phase transitions [1], emergence of new symmetries [2], and Kondo resonances [3]. It is likely that new, yet undiscovered, phenomena can arise from unexplored competing interactions. Today, quantum dots provide controlled and tunable experimental quantum systems to study strong correlation effects. Further, unlike most materials, quantum dots can be modeled using impurity models that can be treated theoretically much more easily. Single quantum dots have been studied extensively, both theoretically and experimentally, which has led to a firm understanding of their Kondo physics [4,5]. More recently, the focus has shifted to multiple quantum dot systems where a richer variety of quantum phenomena become accessible [4,5]. These include emergent symmetries (the symmetry of the low energy physics is larger than the symmetry of the Hamiltonian) [6] and quantum phase transitions [7–9].

In this work we propose a quadruple quantum dot system, that is experimentally realizable, in which three competing interactions determine the low temperature physics: (1) Kondo-like coupling of each dot with its lead, (2) Heisenberg coupling between the dots, and (3) Ising coupling between the dots. Thus, there are two dimensionless parameters with which to tune the competition. The pairwise competing interactions, Kondo-Heisenberg and Kondo-Ising, have both been studied previously. The two impurity Kondo model with a Heisenberg interaction between the impurities shows an impurity quantum phase transition (QPT) from separate Kondo screening of the two spins at small exchange to a local spin singlet (LSS) phase at large exchange. This has received extensive theoretical [7,10,11] and experimental [5] attention. The competition between Kondo and Ising couplings has also been studied theoretically for two impurities [8], including in the quantum dot context [8,9]; however, no experimentally possible realization of this competition has been proposed to date.

Our system consists of four quantum dots and four leads, as shown in Fig. 1(a), with two polarized (spinless)

electrons on the four dots. We find that the system has a rich phase diagram, Fig. 1(b), in terms of the strength of the Heisenberg interaction controlled by t and the Ising interaction controlled by U' . In the absence of the Ising interaction we start in the LSS phase. Upon increasing the Ising

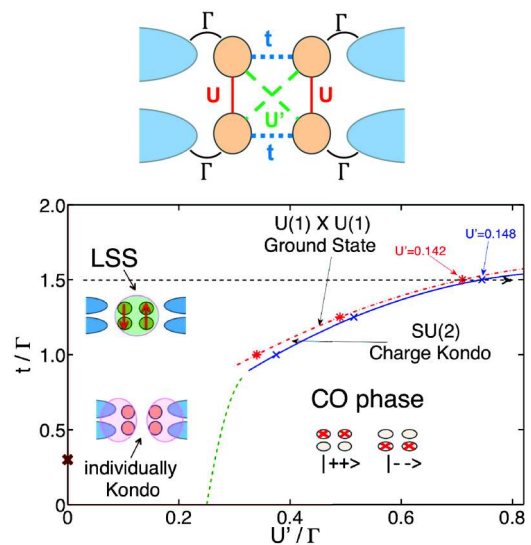


FIG. 1 (color online). (a) Quadruple-dot system. U and U' are electrostatic interactions while t and Γ involve electron tunneling. (b) Ground state phase diagram as a function of the Ising-Kondo tuning U'/Γ and the Heisenberg-Kondo tuning t/Γ , where $U = 3.0$ and $\Gamma = 0.2$. Two distinct phases—charge ordered (CO) and charge liquid—are separated by a KT quantum phase transition [blue crosses (numerical) and green dashed line (schematic)]. Several crossovers lie within the charge-liquid phase. Red stars mark the level crossing where the $U(1) \times U(1)$ state is found (numerical). The charge Kondo region lies between the red and blue lines. “LSS” denotes the local spin singlet state (Heisenberg coupling dominates), while when both Heisenberg and Ising couplings are weak, the system consists of individually screened Kondo states on the left and right. The black dashed line with arrow shows where the calculations for Figs. 2 and 3 have been done.

strength, we find that the system first evolves continuously to a new Kondo-type state with a novel $U(1) \times U(1)$ strong-coupling fixed point, where the symmetry of the low energy physics enhances from left-right Z_2 to $U(1)$. Then there is a crossover to a $SU(2)$ charge Kondo state. Finally, an additional small increase in U' causes a QPT of the Kosterlitz-Thouless (KT) type to a charge-ordered state (CO) (as in Refs. [8,9]) consisting of an unscreened doubly degenerate ground state [12].

Model.—The quantum dots in Fig. 1(a) are capacitively coupled in two ways: U is the vertical interaction (between $L+$ and $L-$; $R+$ and $R-$) and U' is along the diagonal (between $L+$ and $R-$; $L-$ and $R+$). Along the horizontal, there is no capacitive coupling, but there is direct tunneling t (between $L+$ and $R+$; $L-$ and $R-$). Each dot couples to a conduction lead through $\Gamma = \pi V^2 \rho$ where ρ is the density of states of the leads at the Fermi energy. The whole system is spinless. We consider only the regime in which the four dots contain two electrons.

The system Hamiltonian is $H = H_{\text{lead}} + H_{\text{imp}} + H_{\text{coup}}$, where $H_{\text{lead}} = \sum_{i,s,k} \epsilon_k c_{isk}^\dagger c_{isk}$ describes the four conduction leads ($i = L, R$; $s = +, -$), and $H_{\text{coup}} = V \sum_{i,s,k} (c_{isk}^\dagger d_{is} + \text{H.c.})$ describes the coupling of the leads to the dots which produces the Kondo interaction. H_{imp} is the Anderson-type Hamiltonian

$$\begin{aligned} H_{\text{imp}} = & \sum_{i=L,R} \sum_{s=+,-} \epsilon_d d_{is}^\dagger d_{is} + \sum_{i=L,R} U \hat{n}_{i+} \hat{n}_{i-} \\ & + U' (\hat{n}_{L+} \hat{n}_{R-} + \hat{n}_{L-} \hat{n}_{R+}) \\ & + t \sum_{s=+,-} (d_{Ls}^\dagger d_{Rs} + d_{R_s}^\dagger d_{L_s}). \end{aligned} \quad (1)$$

We take $U \gg U'$ so that there is one electron on the left and one on the right.

We can reformulate H_{imp} as an exchange Hamiltonian by noticing that the right-hand (left-hand) sites form a pseudospin: $\vec{S}_i = \sum_{s,s'} d_{si}^\dagger \vec{\sigma}_{ss'} d_{si} / 2$. When $t \ll U$, the effective Hamiltonian for the quantum dots is

$$H_{\text{imp}}^{\text{eff}} \simeq J_H \vec{S}_L \cdot \vec{S}_R - \vec{J}_z S_L^z S_R^z, \quad (2)$$

where $J_H \simeq 4t^2/(U - U'/2)$ and $\vec{J}_z \simeq 2U'$. Thus t controls the strength of the Heisenberg interaction among the dots, and U' controls the Ising coupling. The eigenstates of the impurity site are the usual (pseudo)spin singlet and triplet states, $|S\rangle$, $|++\rangle$, $|--\rangle$, and $|T0\rangle$.

Two limits of our model have been studied previously. First, for $U' = 0$, it becomes the well-known two impurity Kondo model [10,11]. If direct charge transfer is totally suppressed, a QPT occurs between a Kondo screened state (in which the impurities fluctuate between all four states, singlet and triplet) and a LSS [10,11]. When direct tunneling is introduced, the QPT is replaced by a smooth crossover [11]. Second, when $t = 0$, the model has [8,9] a KT-type QPT between the Kondo screened phase at small U' and a CO phase at large U' . The CO phase has an

unscreened doubly degenerate ground state corresponding to $|++\rangle$ and $|--\rangle$.

We solve the model (1) exactly by using finite-temperature world line quantum Monte Carlo (QMC) simulation with directed loop updates [13,14]. We study the regime in which there is a LSS state in the absence of Ising coupling: $4t^2/U > T_K^{L/R}$, where $T_K^{L/R}$ is the Kondo temperature of the left or right pseudospin individually. Taking the leads to have a symmetric constant density of states, $\rho = 1/2D$, with half-band-width $D = 2$, we focus on the case $U = 3$, $\Gamma = 0.2$, and $t = 0.3$. $\beta = 1/T$ is the inverse temperature. As U' is varied [a horizontal scan in Fig. 1(b)], the gate potential is chosen such that $\epsilon_d = -(U + U')/2$, placing the dots right at the midpoint of the two electron regime.

Thermodynamics—As a first step toward distinguishing the different phases, we look at the local charge susceptibility $\chi_c^{\text{loc}} \equiv \int_0^\beta \langle A(\tau) A(0) \rangle d\tau$, where $A \equiv n_{L+} + n_{R+} - n_{L-} - n_{R-}$ and $n_{i,s}$ is the charge density of the dot labeled i, s . Figure 2(a) shows χ_c^{loc} as a function of temperature for different values of U' . The curves show three types of behavior. First, for small Ising coupling ($U' \leq 0.11$), χ_c^{loc} is roughly constant at low T and has a peak at higher temperature. This is the LSS phase. The value of T at which χ_c^{loc} peaks decreases as the energy spacing between the singlet $|S\rangle$ and doublet, $\{|++\rangle, |--\rangle\}$, decreases. Second, at the other extreme, for large Ising coupling ($U' \geq 0.15$), χ_c^{loc} behaves as $1/T$ down to our lowest T . This is a clear signature of the CO phase in which the two charge states $|++\rangle$ and $|--\rangle$ are degenerate. Third, for intermediate values of U' , χ_c^{loc} becomes large and then either decreases slightly at our lowest T or saturates. This behavior can be produced by either a near degeneracy between the singlet and doublet states or by charge

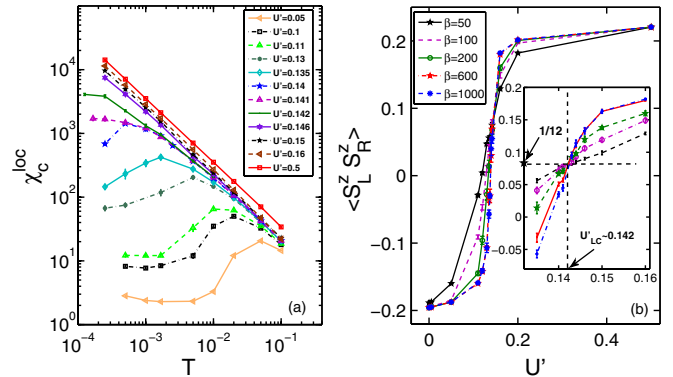


FIG. 2 (color online). (a) Local charge susceptibility as a function of temperature. The power-law behavior of the top three curves indicates the CO phase. The peak and low- T constants in the lowest curves indicate the LSS state. The low- T saturation of the middle curves is due to Kondo-like screening. (b) Pseudospin-pseudospin correlation as a function of U' for different β . Inset: Zoom near the crossing point. The crossing of the singlet and doublet levels occurs at $U'_{\text{LC}} = 0.142$, corresponding to level crossing ($U = 3$, $\Gamma = 0.2$, and $t = 0.3$). The error bars are from statistical error.

Kondo screening of the doublet $\{| + + \rangle, | - - \rangle\}$. As we will see from the conductance data below, the QPT to the CO phase occurs at a value U'_{KT} between 0.146 and 0.15.

To extract the position of the level crossing between $|S\rangle$ and $\{| + + \rangle, | - - \rangle\}$, we calculate the pseudospin correlation function $\langle S_L^z S_R^z \rangle$ as a function of U' for different T [Fig. 2(b)], where $S_i^z = (\hat{n}_{i+} - \hat{n}_{i-})/2$. For $U' = 0$, the ground state is the LSS so that $\langle S_L^z S_R^z \rangle \approx -0.2$ is close to $-1/4$. On the other hand, for large U' , in the CO phase, $\langle S_L^z S_R^z \rangle$ is positive and approaches $1/4$. (The charge fluctuations due to tunneling to the leads causes the values to differ slightly from $\pm 1/4$.) The crossing point of the curves for different temperatures gives the position of the (renormalized) level crossing. The inset shows that it occurs at $\langle S_L^z S_R^z \rangle \approx 1/12$, which is consistent with the isolated-dots limit. The position of the level crossing is, then, $U'_{LC} \approx 0.142$; note that this does *not* coincide with the QPT to the CO phase ($0.146 < U'_{KT} < 0.15$).

Conductance.—Conductance is a crucial observable experimentally. However, the QMC method is only able to provide numerical data for the imaginary time Green function at discrete Matsubara frequencies—the conductance cannot be directly calculated. The zero bias conductance for an impurity model can be obtained [15] by extrapolating to zero frequency. We have recently shown that this method works very well for Anderson-type impurity models in the Kondo region at low temperature [16].

We use this method [12] to find the conductance between the left and right leads as a function of U' for different T ; the results are shown in Fig. 3. For U' small ($U' \leq 0.1$), the conductance is small because the phase shift is nearly zero in the LSS state [10]. For U' large ($U' > 0.15$), the conductance is also small and approaches zero as $U' \rightarrow \infty$, consistent with the argument in Ref. [8]. At intermediate values of U' , there is a strikingly sharp conductance peak near the value of U' where the level crossing occurs. Here, the conductance increases as T decreases and approaches the unitary limit $2e^2/h$ as $T \rightarrow 0$. The position of the conductance peak approaches the level crossing $U' = 0.142$ at low temperature [12]. Its association with the level crossing suggests that this peak comes from fluctuations produced by the degeneracy of $|S\rangle$ and $\{| + + \rangle, | - - \rangle\}$.

A sharp jump appears after the peak: notice that the conductance at $U' = 0.146$ *increases* at lower temperature while that at 0.15 *decreases* [see Figs. 3(b) and 3(c) for clarity]. The latter behavior is the signature of the CO phase, while the former suggests a Kondo-like phase, namely, the dynamic screening of the $\{| + + \rangle, | - - \rangle\}$ doublet. Thus, this sharp jump is associated with the KT QPT from the screened to the CO phase [8], which occurs between $U' = 0.146$ and 0.15.

Effective theory near the level crossing.—To gain insight into the conductance peak, we develop an effective theory near the level crossing. Using Γ/U as a small parameter, we make a Schrieffer-Wolff transformation to integrate out $|T0\rangle$; to include tunneling, processes of order $\Gamma t/U^2$ must

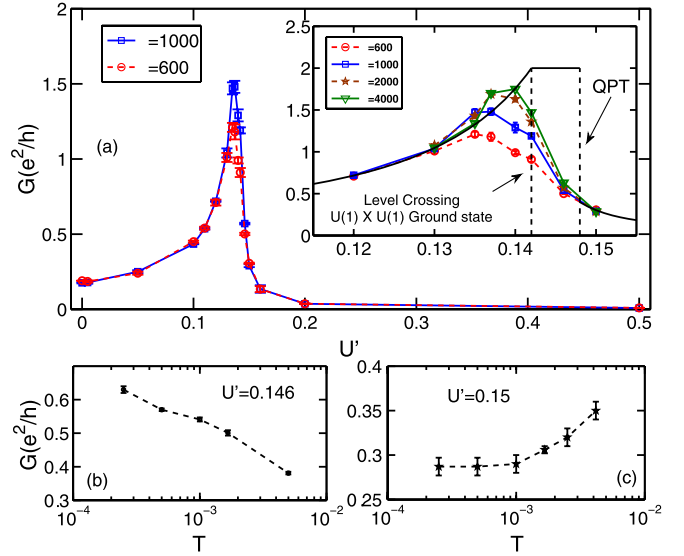


FIG. 3 (color online). (a) Zero bias conductance as a function of U' for two values of β . Inset: Zoom on the peak caused by the $U(1) \times U(1)$ ground state. The $T = 0$ expectation from the effective theory near the level crossing is indicated schematically by the black solid line; the two points of discontinuity (the level crossing and the KT QPT) are marked by dashed lines. (b), (c) Conductance as a function of temperature for $U' = 0.146$ and 0.15, respectively; the opposite trend in these two curves shows that they are on opposite sides of the QPT. The error bars are from both statistical and extrapolation error.

be included [17]. Higher-order terms in Γ/U are neglected. In the leads, only the combinations $\sum_k c_{isk}^\dagger \equiv c_{0,is}^\dagger$ need be considered as these are the locations to which the dots couple. The resulting effective Kondo Hamiltonian reads

$$H_{\text{Kondo}}^{\text{eff}} = J_{\perp}^I (M_+^I S_-^I + M_-^I S_+^I) + 2J_z^I M_z^I S_z^I + J_{\perp}^{\text{II}} (M_+^{\text{II}} S_-^{\text{II}} + M_-^{\text{II}} S_+^{\text{II}}) + 2J_z^{\text{II}} M_z^{\text{II}} S_z^{\text{II}}. \quad (3)$$

The definitions of pseudospins type I and II—the operators M act on the dots and the operators S act on the lead sites—are given in the supplementary material [12]. For $t/U \ll 1$ and particle-hole symmetry, $J_{\perp}^I \simeq J_{\perp}^{\text{II}} \simeq 4V^2/(U + U')$ and $J_z^I \simeq J_z^{\text{II}} \simeq 8V^2 t/(U + U')^2$.

Renormalization effects in $H_{\text{Kondo}}^{\text{eff}}$ can be analyzed using poor man's scaling [18], yielding the scaling equations

$$\begin{aligned} dJ_{\perp}^I/d\ln D &= -2\rho(J_{\perp}^I J_z^I + 3J_{\perp}^{\text{II}} J_z^{\text{II}}) \\ dJ_{\perp}^{\text{II}}/d\ln D &= -2\rho(J_{\perp}^{\text{II}} J_z^{\text{II}} + 3J_{\perp}^I J_z^I) \\ dJ_z^I/d\ln D &= -2\rho[(J_{\perp}^I)^2 + (J_{\perp}^{\text{II}})^2] \\ dJ_z^{\text{II}}/d\ln D &= -4\rho J_{\perp}^I J_{\perp}^{\text{II}}. \end{aligned} \quad (4)$$

Numerical solution of these equations reveals that at a certain value of D all the coupling constants simultaneously diverge. This defines the problem's characteristic energy scale D_0 , which can be considered the Kondo temperature at the level crossing, T_K^{LC} . The coupling constants have a fixed ratio as they diverge: $\lim_{D \rightarrow D_0} J_{\perp}^I : J_{\perp}^{\text{II}} : J_z^I : J_z^{\text{II}} \rightarrow \sqrt{2} : \sqrt{2} : 1 : 1$, suggesting an emergent symmetry in the ground state.

Symmetry analysis.—The six S operators form an $SO(4)$ algebra [12]. However, the six M operators do not; rather they form part of an $SU(3)$ algebra—the missing operators are $|++\rangle\langle--|$ and $|--\rangle\langle++|$ [12]. Since $H_{\text{Kondo}}^{\text{eff}}$ is the product of two objects which generate different algebras, the symmetry of the system must be a subgroup of both $SO(4)$ and $SU(3)$. To study the complete symmetry group of both the bare and fixed-point Hamiltonians, consider the total z component of pseudospins type I and II, $S_{z,\text{tot}}^{\text{I}} \equiv M_z^{\text{I}} + \sum_k S_{z,k}^{\text{I}}$, $S_{z,\text{tot}}^{\text{II}} \equiv M_z^{\text{II}} + \sum_k S_{z,k}^{\text{II}}$. $S_{z,k}^{\text{I/II}}$ is defined by replacing c_0 with c_k in the definition of $S_z^{\text{I/II}}$. One can check that $[S_{z,\text{tot}}^{\text{I}}, H_{\text{lead}} + H_{\text{Kondo}}^{\text{eff}}] = 0$, which gives a (pseudo)spin $U(1)$ symmetry for the bare Hamiltonian. The bare Hamiltonian also commutes with interchanging L and R or interchanging $+$ and $-$. Thus, the symmetry of the bare Hamiltonian is $U(1)_S \times Z_{2,LR} \times Z_{2,+}$ [an irrelevant charge $U(1)$ is ignored].

At the fixed point, $\lim_{D \rightarrow D_0} J_{\perp}^{\text{I}}/J_{\perp}^{\text{II}} \rightarrow 1$ implies that both $S_{z,\text{tot}}^{\text{I}}$ and $S_{z,\text{tot}}^{\text{II}}$ commute with the Hamiltonian: there is an additional $U(1)$ symmetry. Furthermore, note that $\exp(i\theta S_{z,\text{tot}}^{\text{II}})$ generates the $L \leftrightarrow R$ transformation for $\theta = \pi$. Therefore, the $Z_{2,LR}$ symmetry of the bare Hamiltonian is enhanced, becoming an emergent $U(1)$ symmetry. The complete symmetry group at the fixed point (ground state) is $U(1)_S \times U(1)_{LR} \times Z_{2,+}$, where the $Z_{2,+}$ symmetry is irrelevant for the Kondo physics.

Experimental accessibility.—We address two main experimental issues: making of the system and sensitivity to symmetry of parameters. Because of the tunneling t , a small capacitive coupling U_h between dots in the horizontal direction will be present. However, the QPT and $U(1) \times U(1)$ state both still exist provided that $U' - U_h > U'_{\text{KT}}$. This may be achieved by using floating metallic electrodes [19] or an air bridge [20] over the diagonal dots to boost U' . Experimentally, tuning through the transition will result from changing t rather than U' [i.e., a vertical cut in Fig. 1(b)]. When tuning t , U_h will be affected, but the change is small and can be neglected. We need $U \gg U'$ to exclude configurations involving both electrons on the left or right side; the total number of electrons in the four dots can be determined by higher temperature Coulomb blockade experiments.

Possible experimental observation is greatly aided by the fact that not all the symmetries are essential. Those involving the tunneling between the dots or the coupling to the leads, for instance, merely change the coupling constants in the effective Hamiltonian. In both cases, a renormalization-group analysis shows that the $U(1) \times U(1)$ strong-coupling fixed point remains stable. For the QPT, since the asymmetry of t_+ and t_- does not introduce a relevant operator, it does not affect the essential nature of the QPT.

For our scenario, the one crucial symmetry is that $|++\rangle$ and $|--\rangle$ be degenerate; this can be achieved by fine-tuning the gates controlling the levels in the dots. For the

$U(1) \times U(1)$ state we need to have the three-level crossing (by varying one parameter) which gives rise to the effective Hamiltonian Eq. (3). If the detuning is smaller than T_K^{LC} , the crossover is still sharp and the $U(1) \times U(1)$ state remains stable. For the QPT, the detuning $\delta\epsilon$ induces a relevant perturbation in the CO phase [9]. However, a sharp (but continuous) crossover does still occur in the conductance as long as $\delta\epsilon \ll T_K^{\text{LC}}$ and $T \lesssim \delta\epsilon$ [9]. Note that observation of a charge Kondo (CK) effect separately in the left and right dots could be used to zero in on a small $\delta\epsilon$ because of the requirement $\delta\epsilon < T_K^{\text{CK}}$.

We thank G. Finkelstein and A. M. Chang for useful discussions. This work was supported in part by the U.S. NSF Grant No. DMR-0506953.

-
- [1] S. Sachdev, arXiv:0901.4103.
 - [2] R. Coldea *et al.*, *Science* **327**, 177 (2010).
 - [3] P. Coleman, arXiv:cond-mat/0206003.
 - [4] M. Grobis, I. G. Rau, R. M. Potok, and D. Goldhaber-Gordon, arXiv:cond-mat/0611480.
 - [5] A. M. Chang and J. C. Chen, *Rep. Prog. Phys.* **72**, 096501 (2009).
 - [6] T. Kuzmenko, K. Kikoin, and Y. Avishai, *Phys. Rev. Lett.* **89**, 156602 (2002); T. Kuzmenko, K. Kikoin, and Y. Avishai, *Phys. Rev. B* **69**, 195109 (2004).
 - [7] M. Vojta, *Philos. Mag.* **86**, 1807 (2006).
 - [8] M. Garst, S. Kehrein, T. Pruschke, A. Rosch, and M. Vojta, *Phys. Rev. B* **69**, 214413 (2004).
 - [9] M. R. Galpin, D. E. Logan, and H. R. Krishnamurthy, *Phys. Rev. Lett.* **94**, 186406 (2005); *J. Phys. Condens. Matter* **18**, 6545 (2006).
 - [10] I. Affleck, A. W. W. Ludwig, and B. A. Jones, *Phys. Rev. B* **52**, 9528 (1995), and references therein.
 - [11] G. Zaránd, C.-H. Chung, P. Simon, and M. Vojta, *Phys. Rev. Lett.* **97**, 166802 (2006), and references therein.
 - [12] See supplementary material at <http://link.aps.org/supplemental/10.1103/PhysRevLett.105.256801> for text addressing (1) extracting the conductance from the QMC calculations, (2) the shape of the conductance peak, (3) more detail about the effective theory near the level crossing, and (4) an effective theory near the QPT.
 - [13] O. F. Syljuåsen and A. W. Sandvik, *Phys. Rev. E* **66**, 046701 (2002).
 - [14] J. Yoo, S. Chandrasekharan, R. K. Kaul, D. Ullmo, and H. U. Baranger, *Phys. Rev. B* **71**, 201309(R) (2005).
 - [15] O. F. Syljuåsen, *Phys. Rev. Lett.* **98**, 166401 (2007).
 - [16] D. E. Liu, S. Chandrasekharan, and H. U. Baranger, *Phys. Rev. B* **82**, 165447 (2010).
 - [17] Processes of order Γ^n/U^{n+1} produce the same terms in the effective Hamiltonian as Γ/U and $\Gamma t/U^2$ processes, and so do not lead to any essential difference.
 - [18] P. W. Anderson, *J. Phys. C* **3**, 2436 (1970).
 - [19] A. Hubel, J. Weis, W. Dietsche, and K. v. Klitzing, *Appl. Phys. Lett.* **91**, 102101 (2007).
 - [20] E. Girgis, J. Liu, and M. L. Benkheddar, *Appl. Phys. Lett.* **88**, 202103 (2006).

Supplementary Material for “Quantum Phase Transition and Emergent Symmetry in Quadruple Quantum Dot System”

Dong E. Liu, Shailesh Chandrasekharan, and Harold U. Baranger
Department of Physics, Duke University, Box 90305, Durham, North Carolina 27708-0305, USA
 (Dated: October 8, 2010)

In this supplementary material we address (1) extracting the conductance, (2) the shape of the conductance peak, (3) more detail about the effective theory near the level crossing, and (4) an effective theory near the QPT.

I. CONDUCTANCE FROM QUANTUM MONTE CARLO

In this section, we show how to obtain the conductance from quantum Monte Carlo data by the extrapolation method; a longer description, as well as checks, is in Ref. [1]. The quadruple quantum dot system can be mapped to a one-dimensional infinite tight-binding chain as shown in Fig. 1, where a pseudospin is considered on each site (corresponding to + or – in Fig. 1 of the main text). The linear conductance is obtained [1, 2] by extrapolating the conductance at the (imaginary) Matsubara frequencies, $g(i\omega_n)$ with $\omega_n = 2\pi nT$, to zero frequency, $G = \lim_{\omega_n \rightarrow 0} g(i\omega_n)$,

$$g(i\omega_n) = \frac{\omega_n}{\hbar} \int_0^\beta d\tau \cos(\omega_n \tau) \langle P_x(\tau) P_y(0) \rangle, \quad (1)$$

where P_y is the sum of the electron charge density operators to the right of y , $P_y \equiv \sum_{y' \geq y} \hat{n}_{y'}$. Not all combinations of x and y can be used in Eq. (1) because the system is not a physical chain, but only effectively mapped to a chain. Notice that the current through the five bonds closest to the quantum dot sites (labeled $L0$ and $R0$) correspond to the physical current. Therefore, x and y must be chosen from among $\{L1, L0, R0, R1, R2\}$. In addition, left-right symmetry reduces the number of independent combinations. In our calculation, we choose six cases for x and y : $(L0, L0)$, $(R0, R0)$, $(L1, L0)$, $(L1, R0)$, $(L1, R1)$, and $(L0, R0)$. We carry out this extrapolation as in Refs. 2 and 1.

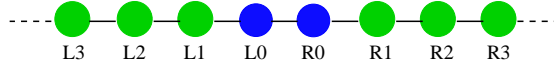


FIG. 1: (color online) The 1D infinite tight-binding chain, where $L0$ and $R0$ mark the impurity (quantum dot) sites.

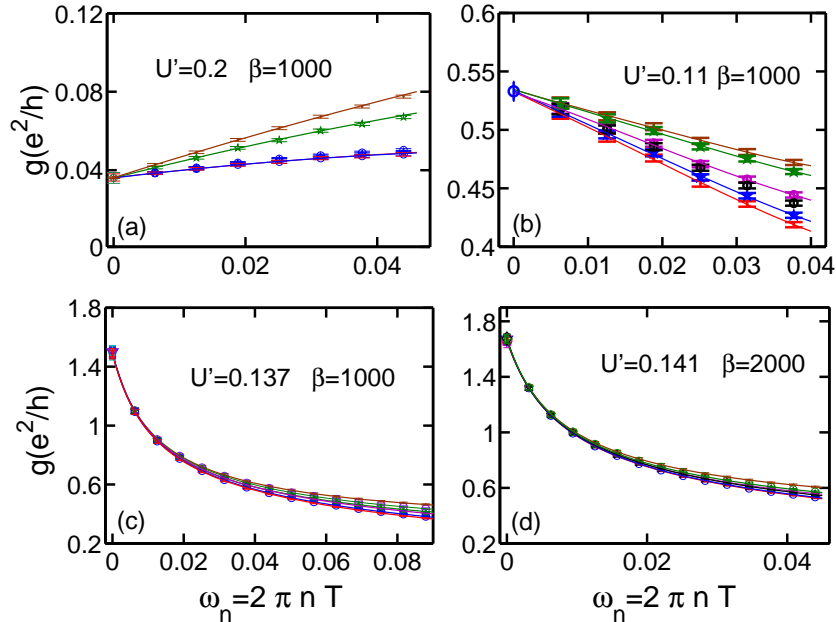


FIG. 2: (color online) Conductance at Matsubara frequencies (symbols) for quadruple dot system and the corresponding fits used to extrapolate to zero frequency (lines). In the calculation, the tunneling $t = 0.3$ and the coupling $\Gamma = 0.2$. The values of U' and β are (a) 0.2, 1000; (b) 0.11, 1000; (c) 0.137, 1000; (d) 0.141, 2000.

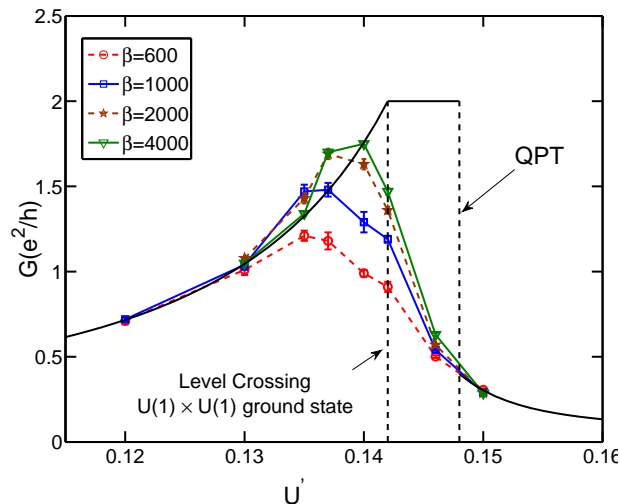


FIG. 3: (color online) Zero bias conductance as a function of U' for different β in the regime of the peak caused by the $U(1) \times U(1)$ ground state. The two vertical dashed lines show the level-crossing and QPT points. The black solid line gives the conductance at zero temperature schematically.

For the CO and LSS regions, the first several QMC data points [$g(i\omega_n)$, $n = 1, \dots, m$, where $m = 4$ to 6 depending on the case] can be fit to a quadratic polynomial, as in Fig. 2(a)(b). For the Kondo regime, the first 14 QMC data points [$g(i\omega_n)$, $n = 1 \dots 14$] are fit to a series of rational polynomial functions [see Fig. 2(c)(d) for examples]. The conductance is the average of the different extrapolation results, and the error bar corresponds to the maximum spread. For all of the cases studied in this work, the extrapolation appears to be straight forward and reliable (for cases in other systems for which the extrapolation does not work well, see Ref. 1).

II. PEAK OF CONDUCTANCE NEAR RESONANCE

Fig. 3 shows that the conductance peak approaches the level-crossing point as the temperature approaches zero, as expected from the $T = 0$ theory, but that the peak is not at the level-crossing point at non-zero T . This shift in the peak position can be understood as follows. When the parameter U' increases toward the level-crossing point $U'_{LC} \approx 0.142$, the singlet $|S\rangle$ is the ground state of the dots, and the level splitting Δ between $|S\rangle$ and the doublet $\{|+\rangle, |-\rangle\}$ states decreases to zero at U'_{LC} . Following the argument in Ref. 3 concerning the effect of a magnetic field on the usual quantum dot Kondo effect, we expect that the effect of the level splitting Δ at zero temperature should be similar to that of the temperature at zero level splitting, though $G(\Delta/T_K, T = 0)$ and $G(T/T_K, \Delta = 0)$ may have different universal forms. For finite $\Delta \ll T$, G can be approximated by $G(T/T_K, \Delta = 0)$ which saturates at $2e^2/h$ at low temperature. On the other hand, at $T = 0$, $G(T = 0, \Delta) < 2e^2/h$ (because the LSS has a substantial weight in the ground state). Therefore, the conductance $G(T/T_K, \Delta)$ may show a peak at non-zero T , and does so for, e.g., $U' = 0.135$ in Fig. 3. Similarly, for fixed $T \neq 0$, $G(\Delta/T_K)$ may peak at non-zero Δ . In summary, although the conductance peaks at $\Delta = 0$ for $T = 0$, at non-zero temperature, $G(U')$ may show a peak at $U' < 0.142$ corresponding to finite level splitting Δ .

III. EFFECTIVE THEORY NEAR THE LEVEL CROSSING

The definition of the S operators in Eq. (3) of the main text is

$$\begin{aligned}
 S_{\pm}^I &= (c_{0,L\pm}^{\dagger} c_{0,L\mp} - c_{0,R\pm}^{\dagger} c_{0,R\mp}) \\
 S_z^I &= \frac{1}{2} \sum_{i=L,R} (c_{0,i+}^{\dagger} c_{0,i+} - c_{0,i-}^{\dagger} c_{0,i-}) \\
 S_{\pm}^{II} &= (\pm c_{0,R\pm}^{\dagger} c_{0,L\mp} \mp c_{0,L\pm}^{\dagger} c_{0,R\mp}) \\
 S_z^{II} &= \frac{1}{2} \sum_{s=+,-} (c_{0,Ls}^{\dagger} c_{0,Rs} + c_{0,Rs}^{\dagger} c_{0,Ls}).
 \end{aligned} \tag{2}$$

The S operators satisfy the following commutation relations:

$$\begin{aligned}
[S_+^I, S_-^I] &= 2S_z^I & [S_z^I, S_\pm^I] &= \pm S_\pm^I \\
[S_+^{II}, S_-^{II}] &= 2S_z^{II} & [S_z^{II}, S_\pm^{II}] &= \pm S_\pm^{II} \\
[S_+^I, S_-^{II}] &= 2S_z^I & [S_z^I, S_\pm^{II}] &= \pm S_\pm^{II} \\
[S_+^{II}, S_-^I] &= 2S_z^{II} & [S_z^{II}, S_\pm^I] &= \pm S_\pm^I \\
[S_+^I, S_+^{II}] &= 0 & [S_-^I, S_-^{II}] &= 0 & [S_z^I, S_z^{II}] &= 0.
\end{aligned} \tag{3}$$

These relations generate the $SO(4)$ algebra, so the six S operators form an $SO(4)$ algebra. However, the six M operators do *not* form an $SO(4)$ algebra. If the standard basis for the fundamental representation of $SU(3)$ is F_i , $i = 1, 2, \dots, 8$ [4], the definition of the six M operators in Eq. (3) of the main text is

$$\begin{aligned}
M_+^{I/II} &= \sqrt{2}(|++\rangle\langle S| \mp |S\rangle\langle --|) = (M_-^{I/II})^\dagger \\
M_z^I &= |++\rangle\langle ++| - |--\rangle\langle --| \\
M_z^{II} &= |++\rangle\langle ++| + |--\rangle\langle --| - 2|S\rangle\langle S|,
\end{aligned} \tag{4}$$

which can be written as the linear combinations

$$\begin{aligned}
M_z^I &= F_3, & M_z^{II} &= (2/\sqrt{3})F_8, \\
M_+^I &= (F_4 + iF_5 - F_6 + iF_7)/\sqrt{2}, & M_-^I &= (F_4 - iF_5 - F_6 - iF_7)/\sqrt{2}, \\
M_+^{II} &= (F_4 + iF_5 + F_6 - iF_7)/\sqrt{2}, & M_-^{II} &= (F_4 - iF_5 + F_6 + iF_7)/\sqrt{2}.
\end{aligned} \tag{5}$$

The two missing operators $|++\rangle\langle --|$ and $|--\rangle\langle ++|$ can be written as

$$|++\rangle\langle --| = F_1 + iF_2, \quad |--\rangle\langle ++| = F_1 - iF_2. \tag{6}$$

Therefore, the six M operators combined with the two missing operators form an $SU(3)$ algebra.

Up to order Γ/U , there is no direct process which leads to $|++\rangle \Leftrightarrow |--\rangle$. The only path leading to $|++\rangle \Leftrightarrow |--\rangle$ is via the singlet state as an intermediary: $|++\rangle \Leftrightarrow |S\rangle \Leftrightarrow |--\rangle$. When higher-order terms $(\Gamma/U)^2$ are considered, the four electron hopping terms do produce a direct $|++\rangle \Leftrightarrow |--\rangle$ process:

$$H_{\text{flip}}^{\text{eff}} = A \sum_{k, k', q, q'} \left(|++\rangle\langle --| c_{kL}^+ c_{k'L}^+ c_{qR}^+ c_{q'R}^+ + \text{h.c.} \right). \tag{7}$$

Since $H_{\text{flip}}^{\text{eff}}$ is comprised of four electron operators, its naive scaling dimension is negative, suggesting that $H_{\text{flip}}^{\text{eff}}$ is irrelevant. To check this, consider the one-loop RG equations. The scaling equations for the system combining $H_{\text{flip}}^{\text{eff}}$ with $H_{\text{Kondo}}^{\text{eff}}$ [Eq. (3) of the main text] consist of the original four equations in Eq. (4) of the main text plus one additional equation:

$$\frac{dA}{d \ln D} = -2\rho J_\perp^I A. \tag{8}$$

Solving these five equations numerically with $J_\perp^I > 0$, we find that the coupling A flows to 0 for any initial value. Therefore, $H_{\text{flip}}^{\text{eff}}$ is an irrelevant operator in the strong coupling phase, which confirms the naive scaling-dimension analysis.

Finally, we have studied the effect of asymmetric parameters on the stability of the $U(1) \times U(1)$ fixed point in the RG sense. We assume that the low energy effective Hamiltonian has the same structure as in Eq. (3) of the main text but allow each coupling parameter to be different—10 couplings in all rather than the 4 analyzed in the paper. Poor man's scaling yields RG equations for these 10 couplings [the analog of Eq. (4)], and numerical solution of these equations shows that the flow is toward the $U(1) \times U(1)$ state for all values (as long as they are antiferromagnetic). This seems natural given the scaling of the simple spin- $\frac{1}{2}$ Kondo model. Thus, experimental asymmetries in these parameter are irrelevant.

IV. EFFECTIVE THEORY NEAR THE QPT

To study the physics near the KT quantum phase transition, we develop a low energy effective theory closely following Refs. 5 and 6. First, consider the effective Hamiltonian in the large U' limit without tunneling, and note

that the energy of $|S\rangle$ is much higher than that of $\{|++\rangle, |--\rangle\}$. Using Γ/U as a small parameter, we make a Schrieffer-Wolff transformation to integrate out $|T0\rangle$ and $|S\rangle$; higher-order terms are neglected. The resulting fixed point Hamiltonian is

$$H_{\text{CO}}^{\text{eff}} = \sum_{k,s=L/R,\sigma=+/-} \epsilon_{ks\sigma} c_{ks\sigma}^+ c_{ks\sigma} + K \sum_{kk'\sigma} (\hat{n}_{L\sigma} + \hat{n}_{R\sigma} - 1) c_{ks\sigma}^+ c_{k'\sigma} . \quad (9)$$

The ground state corresponds to a *charge ordered state* with two-fold degeneracy, $\{|++\rangle, |--\rangle\}$: the two electrons are frozen in either the upper two quantum dots or the lower dots. The charge order can be screened by $H_{\text{flip}}^{\text{eff}}$ given in Eq. (7). The model here is very similar to that for the orthogonality catastrophe in the x-ray edge problem [7, 8], as pointed out in Refs. 5 and 6; we briefly summarize their argument here.

The charge ordered state can be flipped by the operator $\hat{f} \equiv |++\rangle\langle --| c_{kL-}^+ c_{k'L+} c_{qR-}^+ c_{q'R+}$. According to Hopfield's rule of thumb [9], the correlation function in the charge-ordered phase is given by

$$\langle \hat{f}^+(t) \hat{f}(0) \rangle_{H_{\text{CO}}^{\text{eff}}} \sim t^{-\alpha} \quad \text{where} \quad \alpha = \sum_{i=L+,L-,R+,R-} (\Delta n_i)^2 \quad (10)$$

is related to the change in occupation Δn_i of each dot. Δn_i can be expressed in terms of the conduction band phase shift δ through the Friedel sum rule; therefore, the anomalous exponent can be related to δ ,

$$\alpha = \sum_{i=L+,L-,R+,R-} (\Delta n_i)^2 = 4 \left(\frac{2\delta}{\pi} - 1 \right)^2 . \quad (11)$$

In a 1D problem such as ours, the power-law decay of correlations in Eq. (10) leads to the criteria

$$\begin{cases} \alpha/2 > 1 & \text{irrelevant} & \text{Charge Ordered state} \\ \alpha/2 < 1 & \text{relevant} & \text{Charge Kondo state} \\ \alpha/2 = 1 & \text{marginal} & \text{Critical Point} \end{cases}$$

because of the possible infrared (long time) singularity. Thus the criterion for the critical point separating the charge-ordered and charge-Kondo states is

$$2 \left(\frac{2\delta_c}{\pi} - 1 \right)^2 = 1 \implies \delta_c = \frac{\pi}{2} \left(1 - \frac{1}{\sqrt{2}} \right) . \quad (12)$$

The phase shift δ depends on the coefficient K of the potential scattering term in $H_{\text{CO}}^{\text{eff}}$, while K itself depends on U , U' , and Γ . Therefore, the phase shift is a function of U , U' , and Γ , and

$$\delta_c(U, U'_{\text{KT}}, \Gamma) = \frac{\pi}{2} \left(1 - \frac{1}{\sqrt{2}} \right) \implies U'_{\text{KT}} = f(U, \Gamma) . \quad (13)$$

So, when $U > U'_{\text{KT}}$, we have $\alpha > 2$, $H_{\text{flip}}^{\text{eff}}$ is irrelevant, and the system is in the charge-ordered phase with a two-fold degenerate ground state. However, when $U < U'_{\text{KT}}$, $\alpha < 2$, $H_{\text{flip}}^{\text{eff}}$ is relevant, and so this four electron hopping operator produces $|++\rangle \leftrightarrow |--\rangle$ which screens the charge-ordered state to form the charge-Kondo state. There is a KT-type quantum phase transition [5, 6] at $U' = U'_{\text{KT}}$.

In contrast to Refs. 5 and 6, we must consider the influence of the tunneling t on the QPT (i.e. direct tunneling between $L+$ and $R+$, and between $L-$ and $R-$). To include tunneling, processes of order $\Gamma t/U^2$ need to be considered [10]. The low energy effective Hamiltonian in the charge-ordered phase becomes

$$\begin{aligned} H_{\text{COt}}^{\text{eff}} = & \sum_{k,s=L/R,\sigma=+/-} \epsilon_{ks\sigma} c_{ks\sigma}^+ c_{ks\sigma} + K \sum_{kk'\sigma} (\hat{n}_{L\sigma} + \hat{n}_{R\sigma} - 1) c_{ks\sigma}^+ c_{k'\sigma} \\ & + \widetilde{K}_t \sum_{k,k',\sigma} (\hat{n}_{L\sigma} + \hat{n}_{R\sigma} - 1) (c_{kL\sigma}^+ c_{k'R\sigma} + c_{kR\sigma}^+ c_{k'L\sigma}) . \end{aligned} \quad (14)$$

The contribution of the tunneling merely adds the possibility of potential scattering between the electrons in the left and right leads; note that the dependence on the filling of the four dots, either $|++\rangle$ or $|--\rangle$, is the same. Thus, tunneling does not introduce a charge order flip process, but does contribute to the phase shift experienced by the lead electrons when the dot flips. We expect, then, that t does not affect the essential physics of the charge-ordered

phase and QPT. We should check, however, whether the tunneling leads to a relevant process in addition to $H_{\text{flip}}^{\text{eff}}$ which can screen the charge order. The lowest order screening terms induced by tunneling are

$$\hat{f}_1 = |++\rangle\langle--|c_{kL}^+c_{k'L+}c_{qR}^+c_{q'L+}, \quad \hat{f}_2 = |++\rangle\langle--|c_{kL}^+c_{k'L+}c_{qL}^+c_{q'L+}. \quad (15)$$

Following the arguments given above, we find that the anomalous exponent for \hat{f}_1 is $\alpha/2 = 2(2\delta/\pi - 1)^2 + 1 \geq 1$, while that for \hat{f}_2 is $\alpha/2 = 2(2\delta/\pi - 1)^2 + 2 > 1$. Therefore, both \hat{f}_1 and \hat{f}_2 are irrelevant operators in the charge ordered phase. The tunneling does not affect the essential physics (i.e. the quantum phase transition) of the system. Its influence is only felt through the phase shift δ which depends on the tunneling t . U'_{KT} , then, is a function of U , Γ , and now t . Thus, the tunneling t *does* affect where the QPT occurs (Fig. 1 in the main text); in particular, to observe the QPT in experiments, t can be tuned instead of or in addition to the interaction U' .

In the quadruple dot system, the tunneling t_+ through the upper dots and t_- through the lower dots are two independent tunable parameters. Although one can measure the conductance as a function of both t_+ and t_- , it is still crucial to study how the tunneling asymmetry affects the physics of the system [QPT and $U(1) \times U(1)$ Kondo state]. It is easy to check that the $U(1) \times U(1)$ state is robust against this asymmetry: we have looked at the RG flow near the $U(1) \times U(1)$ fixed point for $t_+ \neq t_-$ and checked that the fixed point is stable. For the QPT, if $t_+ \neq t_-$, one has $\widetilde{K}_{t_+} \neq \widetilde{K}_{t_-}$. Since the phase shift δ depends on \widetilde{K}_t , $\widetilde{K}_{t_+} \neq \widetilde{K}_{t_-}$ results in $\delta_+ \neq \delta_-$. We can assume $\delta_+ = \delta + \Delta$ and $\delta_- = \delta - \Delta$, where Δ is a small quantity depending on $\delta_+ - \delta_-$. In this case, Eq. (12) above becomes

$$\left(\frac{2(\delta_c + \Delta)}{\pi} - 1\right)^2 + \left(\frac{2(\delta_c - \Delta)}{\pi} - 1\right)^2 = 1. \quad (16)$$

If Δ is not large ($8\Delta^2/\pi^2 < 1$), this equation has a real solution which shows that the QPT does still exist, though its position will be affected by Δ . If Δ is large ($8\Delta^2/\pi^2 > 1$), the equation above does not have a real solution, and there is no QPT. Therefore, as long as the asymmetry $|\delta_+ - \delta_-|$ is not too large, the essential nature of QPT will not be affected.

-
- [1] D. E. Liu, S. Chandrasekharan, and H. U. Baranger, arXiv:1007.5280 (2010).
[2] O. F. Syljuåsen, Phys. Rev. Lett. **98**, 166401 (2007).
[3] L. I. Glazman and M. Pustilnik, in *Nanophysics: Coherence and Transport*, edited by H. Bouchiat, Y. Gefen, S. Gueron, G. Montambaux, and J. Dalibard (Elsevier, 2005), pp. 427–478, arXiv:cond-mat/0501007.
[4] M. E. Peskin and D. V. Schroeder, *An Introduction to Quantum Field Theory* (Westview Press, 1995), p. 502.
[5] M. Garst, S. Kehrein, T. Pruschke, A. Rosch, and M. Vojta, Phys. Rev. B **69**, 214413 (2004).
[6] M. R. Galpin, D. E. Logan, and H. R. Krishnamurthy, Phys. Rev. Lett. **94**, 186406 (2005), and J. Phys.: Condens. Matter **18**, 6545 (2006).
[7] P. W. Anderson, Phys. Rev. Lett. **18**, 1049 (1967).
[8] G. D. Mahan, *Many-Particle Physics* (Kluwer Academic/Plenum Publishers, New York, 2000), 3rd ed., pp. 612-621.
[9] J. J. Hopfield, Comments Solid State Phys. **2**, 40 (1969).
[10] Processes of order $\Gamma t^n/U^{n+1}$ produce the same terms in the effective Hamiltonian as Γ/U and $\Gamma t/U^2$ processes, and so do not lead to any essential difference.